



Time-dependent drivers explain correspondence between wastewater and clinical COVID-19 data

Daniele Sartirano^{a,b,*}, Niel Hens^{b,c}, Claudio Lubello^a

^a University of Florence, Department of Civil & Environmental Engineering, Florence, Tuscany, Italy

^b University of Hasselt, Data Science Institute, Hasselt, Limburg, Belgium

^c University of Antwerp, Centre for Health Economic Research and Modeling Infectious Diseases (CHERMID), Vaccine and Infectious Disease Institute, Antwerp, Belgium

ARTICLE INFO

Keywords:

COVID-19
Generalized additive mixed model
Wastewater
Clinical tests accuracy
Viral prevalence

ABSTRACT

Wastewater-based epidemiology has garnered increasing attention during the COVID-19 pandemic due to its potential for accurate and cost-effective population-level surveillance. In this study, we analyzed wastewater samples collected from six wastewater treatment plants in Tuscany, Italy, between April 2022 and March 2023. We compared SARS-CoV-2 RNA concentrations in wastewater with the number of positive COVID-19 tests provided by the Italian Ministry of Health and observed significant discrepancies between the two throughout the whole time window considered, with viral load ranging from 4 up to 8 orders of magnitude higher than clinical tests. These inconsistencies tend to increase with time by 1–2 orders of magnitude. To investigate the underlying causes of these discrepancies, we developed a Generalized Additive Mixed Model incorporating both clinical testing intensity (using the number of tests performed and the positivity ratio as proxies for testing accuracy) and viral subvariant prevalence. Our results indicate that variations in clinical testing intensity introduce changes in the relationship between their estimates and the wastewater-based time series, with an effect that is more than double the impact of Omicron subvariants. Shifts in viral subvariants produce systematic changes in the wastewater signal with an effect more than double the one of clinical tests. When not taken properly into account, they effectively act as a bias in the relationship between measured concentrations and case numbers.

1. Introduction

The SARI project (Sorveglianza Ambientale dei Reflui in Italia, Environmental Surveillance of Wastewater in Italy) is a national environmental monitoring network coordinated by the Italian National Institute of Health.¹ Established during the COVID-19 pandemic, its objectives are twofold: to enable retrospective epidemiological studies through wastewater data analysis and to explore the feasibility of wastewater-based epidemiology (WBE) as a permanent surveillance tool for infectious diseases in Italy.

Projects similar to SARI were started in several countries, with surveillance dashboards in 31 countries as shown by the World Health Organization.² WBE has emerged as a promising approach for public health surveillance, offering early detection capabilities [1–3] at relatively low cost [4,5]. Several studies have reported strong correlations between SARS-CoV-2 RNA concentrations in wastewater and clinically confirmed case numbers [6–10].

In the European Union, Directive 2024/3019 concerning urban wastewater treatment [11] has recently stressed on the importance of wastewater-based surveillance to protect public health following the One Health approach. The directive encourages the institution of wastewater-based surveillance program for preventive purposes, requiring member states to monitor wastewater during health emergencies. To pursue this goal, we need to gain a better understanding of how noise factors affect the relationship between wastewater and clinical test data.

Findings pertaining the correlation between wastewater data and positive clinical test can be sometimes limited by several noise factors affecting both wastewater and clinical test data. The limitations of clinical testing, including under-detection of asymptomatic cases and dependence on healthcare system logistics, have been well documented [12,13]. For wastewater data, two main sources of variability are commonly addressed: dilution effects due to changes in wastewater

* Corresponding author at: University of Florence, Department of Civil & Environmental Engineering, Florence, Tuscany, Italy.
E-mail addresses: daniele.sartirano@unifi.it, daniele.sartirano@uhasselt.be (D. Sartirano).

¹ <https://www.salute.gov.it/portale/nuovocoronavirus/dettaglioNotizieNuovoCoronavirus.jsp?id=4953>

² <https://data.who.int/dashboards/covid19/wastewater>

flow, often mitigated through normalization with proxies such as *Pep-per Mild Mottle Virus* or flow rate [14–16], and degradation of viral genomic material within the sewage system [17], typically modeled as a first-order decay process [18–20].

Xiao et al. working on wastewater samples from the Greater Boston area (2.3 million people monitored) from 2020–2021 noted that the ratio between wastewater copy numbers of SARS-CoV-2 genetic material and clinical cases is time-dependent [21]. The authors consider the shifts in the ratio as due to clinical test accuracy and changes in demography and propose this signal as a way to monitor the former. A cohort study on 268 counties in 22 US States also found that during the 2020–2022 time window the association between SARS-CoV-2 wastewater metrics and clinical tests positives declined, attributing this trend to the adoption of home testing and the effect of vaccination [22]. Schill et al. working on Californian data between 2020 and 2023, found a correlation between the time-dependent relationship shift and both the clinical test rate and the presence of a different viral variant [23].

Another factor whose impact remains underexplored is viral variant prevalence. Different SARS-CoV-2 variants have been shown to produce varying viral loads in infected individuals, which in turn influences viral shedding and affects the concentrations measured in wastewater [24,25].

In this study, we analyzed SARS-CoV-2 RNA concentrations measured at the inlets of six wastewater treatment plants (WWTPs) across Tuscany between April 2022 and March 2023. We compared these concentrations to estimated infection trends derived from clinical test data using the model proposed by Hetebrji et al. [26] which they applied for the Netherlands. While we expected to observe a consistent correlation, our results indicated a substantially weaker association than typically reported in the literature, with notable temporal fluctuations, particularly from January 2023 onwards.

To better understand the factors underlying these discrepancies, we considered the factors that can affect the relationship between clinical and wastewater signals. To disentangle those contributions, we constructed a Generalized Additive Mixed Model (GAMM, [27]) to analyze the absolute differences between clinical testing trends and wastewater concentrations. Our aim is to use this approach to identify the main drivers behind the discrepancy we observe and to quantify their impact.

Our results highlight the need to account for subvariant-specific shedding patterns and testing practices when interpreting wastewater data for epidemiological surveillance. Importantly, they give a more precise perspective of the underlying phenomena and to confirm solidly the hypotheses found in literature. In addition, our work shows how the viral prevalence effect is relevant even within the same viral variant (Omicron, in this case), therefore considering subvariants belonging to the same variant of concern. Such considerations are essential for improving the accuracy and reliability of WBE as a non-traditional data source for monitoring infectious diseases.

2. Materials & methods

2.1. Wastewater data

We extracted wastewater samples at the inlets of six different WWTPs in the Tuscany region of Italy. These plants serve the cities of Florence (San Colombano, 516,197 people), Prato (Baciacavallo, 174,023 people), Pistoia (Pistoia Central, 56,121 people), Arezzo (Casolino, 62,771 people), Siena (Tressa, 49,089 people), and Grosseto (San Giovanni Pianetto, 61,640 people). For each sewage network, we delineated the catchment area by applying a 200 m buffer to the network links using QGIS software and estimated the population served by referencing resident population data from the National Statistics Institute (ISTAT).

We collected sewage samples weekly from plants serving fewer than 100,000 people and bi-weekly on two consecutive days from the larger

plants. Each sample was composite, comprising 24 hourly extractions from the wastewater flow starting at 9 a.m. We recorded flow rate estimates within the same timeframe using a flow meter. Our data collection spanned from 07/04/2022 to 23/03/2023.

A more in detail description of the sampling process and the methodology that was utilized to measure the RNA concentration in each sample is contained in Morecchiato et al. [28]. We derived the trend for each WWTP from the raw wastewater concentration data following the methods described by Hetebrji et al. [26].

2.2. Clinical test data

We obtained clinical test data for the study period from the official repository of the Civil Protection Department.³ The dataset reports the total number of clinical tests analyzed aggregated at the Tuscany level (administrative level 1), while it provides the number of positive cases detected at the finer province level (administrative level 2). To derive plant-level values, we assumed a homogeneous spatial distribution and normalized the data based on the fraction of the regional or provincial population residing within each catchment area. This assumption implies that, during the 2022–2023 period, the COVID-19 pandemic was sufficiently widespread that spatial variation in infection levels was negligible. Under this assumption, the number of infected individuals at the plant level can be estimated as a fraction of the corresponding provincial total, with this fraction approximated by the share of the provincial population residing within the plant's catchment area.

Throughout the timeframe of this study, testing policies remained largely constant. In Italy, the state of emergency declared for the COVID-19 pandemic ended on 31 March 2022, one week before the start of sampling. Consequently, no non-pharmaceutical interventions were in place during the study period, except for the European green certificate requirement for workers over 50 years old to access their workplace, which ended on 1 May 2022. Individuals obtained this certificate after receiving at least the first vaccine booster dose.

We derived the COVID-19 incidence trend in each catchment area by smoothing the raw clinical data using the EpiLPS library [29].

We retrieved viral subvariant prevalence data at the national level from the Tess-Y dataset provided by the European Centre for Disease Control (ECDC).⁴ In the same vein as per clinical tests, we assume that there is not statistically meaningful difference between the prevalence among people living in each plant's catchment area and the national data. Throughout the sampling period, the Omicron variant accounted for at least 95% of total cases on any given day. The only non-Omicron subvariant detected was B.1.617.2, a Delta subvariant. The ECDC grouped minor subvariants under the category "Other", while tests yielding no clear result were reported as "UNK" (unknown). Subvariant data were unavailable after 29 January 2023.

We are aware that clinical tests suffer from severe underreporting and that many advocate for the usage of alternative data sources, such as the number of deceased or hospitalized paired with mathematical models [30–32]. However, we chose to focus on the clinical tests only since they are more closely linked to SARS-CoV-2 RNA concentration in wastewater, without the need to incorporate the epidemiological delay related to the deceased estimate alongside the ones already affecting clinical tests and wastewater data. This additional modeling burden would constitute an additional source of noise for our approach, which already faces limitations due to the coarseness of the wastewater dataset. Finally, we think that comparing sources as close as possible within the epidemiological evidence pyramid [33] is the most straightforward choice.

However, we have also applied the model using the number of deceased, collected from the same Civil Protection Department dataset. Results are discussed in Appendix A.

³ <https://github.com/pcm-dpc/COVID-19>

⁴ <https://www.ecdc.europa.eu/en/publications-data/data-virus-variants-covid-19-eueea>

2.3. Data analysis and feature selection

We began our analysis by applying the model proposed by Hetebrji et al. to evaluate the correlation between SARS-CoV-2 trends estimated from wastewater concentrations and those derived from clinical testing data. This model pools all data into a unified fitting procedure, potentially improving robustness by leveraging shared structure across sites. However, despite this adjustment, the wastewater-based estimates remained noticeably different from the clinical trends across all WWTPs.

To quantify the discrepancy, we computed both the absolute and relative differences between the two time series. Since both metrics produced similar results, we focus on the absolute difference for the remainder of the study. The difference for plant p at day t is defined as:

$$D_{p,t} = \left| \log_{10} C_t - \hat{W}_{p,t} \right| = \left| \log_{10} C_t - \log_{10} \frac{\text{copies}_{p,t}}{100,000} \right| = \left| \log_{10} \frac{100,000 * C_t}{\text{copies}_{p,t}} \right| \quad (1)$$

with $D_{p,t}$ as the absolute difference for plant p at day t , C_t as the number of positive clinical tests reported on day t , $\hat{W}_{p,t}$ as the Hetebrji et al. model estimate for plant p on day t , $\text{copies}_{p,t}$ as the number of SARS-CoV-2 genomic copies found in the wastewater from plant p on day t .

It should be noted that this comparison is based on same-day estimates from both data sources, as no lag between wastewater and clinical test data was identified. However, this finding is likely influenced by the temporal granularity of the wastewater data. In particular, weekly measurements do not allow for the detection of sub-weekly lags, even if such lags are present. Nonetheless, given the available data and the structure of the analysis, this definition of the difference appears to be the most appropriate.

We hypothesize that the difference remains constant over time. Although the numerical values of viral load and the number of infected individuals may differ, wastewater measurements and clinical testing data are expected to capture the same underlying COVID-19 pandemic dynamics. Accordingly, both indicators should exhibit synchronous increases and decreases, yielding a constant absolute difference. However, as shown in Fig. 3, this expectation is not supported by the data. This suggests that the mechanisms underlying the discrepancy between clinical testing and wastewater signals are time-dependent. Furthermore, comparison of wastewater trends across catchment areas, based on their absolute differences, reveals a high degree of similarity, indicating that the underlying processes are consistent across catchments and thus spatially homogeneous.

For additional safety, we also tried to use the relative difference in place of the absolute difference. Since results were extremely close, we will focus on the absolute difference only.

We subsequently investigated the influence of factors commonly identified in the literature as potential drivers of such effects, while imposing the constraint that any plausible explanation must exhibit both temporal variability and spatial homogeneity in the context of the COVID-19 pandemic.

We first considered changes in legislation affecting testing, or public health guidelines as potential causes, but we verified that no major policy changes occurred during the observation period [34]. Therefore, we excluded this explanation. We did not, however, take into account the possibility of a self-induced behavioral change in the population.

Next, we tested for statistical correlations, using both Pearson and Spearman methods, between the absolute difference and several related factors. We began with environmental and infrastructural factors, especially dilution effects, as we measure viral concentration in wastewater. Population shifts and rainfall are the two primary drivers of dilution. However, we had already normalized our data using daily average flow rates to account for population-related changes, and this correction

should mitigate such effects. Specifically, a larger population means a higher water consumption and therefore a higher flow rate. Regarding rainfall, in addition to dilution, it should also reduce signal degradation by accelerating wastewater transit through the network, thus shortening exposure to the chemical environment in the sewage pipes that breaks down viral RNA. Nevertheless, we found no significant correlation between rainfall volume in the catchment area and the observed differences, further weakening the rain effect hypothesis. Nevertheless, we later tried to introduce rain as a feature in the GAMM. However, it was always discarded during the fitting process and consequently the variable is not present in any of the final models.

We then turned our attention to epidemiological variables. Specifically, we investigated whether changes in clinical testing accuracy could account for the discrepancy. Since direct estimates of clinical test accuracy were unavailable, we used the test positivity rate (i.e., the ratio of detected positives to total tests conducted) as a proxy. We found that this variable correlated with the absolute difference, indicating that variations in testing practices or test-seeking behavior, despite the absence of changes in testing regulations, played a role in the misalignment between the wastewater and clinical datasets.

Finally, we explored the role of viral subvariant prevalence. Prior literature suggests that different SARS-CoV-2 variants may exhibit distinct shedding profiles, thereby altering the concentration of viral material detected in wastewater. Our analysis confirmed that the difference correlated with the prevalence of specific subvariants, particularly those showing clear dominance during the study period.

Given these findings, we constructed a GAMM to quantify the contribution of these factors — clinical testing patterns and viral subvariant prevalence — to the observed discrepancy. While correlation tests established the presence of associations, the Generalized Additive Mixed Model (GAMM) allowed us to assess the relative importance and temporal dynamics of each variable in a statistically rigorous framework.

2.4. GAMM

We constructed a GAMM for each wastewater treatment plant using a set of selected explanatory variables. On the clinical testing side, we included: the base-10 logarithm of the number of positive cases per 100,000 people, the base-10 logarithm of the total number of tests performed daily, and the positivity rate (i.e., the ratio between the two). On the biological side, we incorporated the prevalence of viral subvariants, as well as the “Other” and “Unknown” categories reported in the ECDC dataset. Since the dataset provides no subvariant information beyond 29 January 2023, we restricted model fitting to data collected up to that date.

To explore the relationship between these variables and the observed differences, we evaluated all possible modeling configurations for each factor: (1) excluding the variable entirely, (2) modeling its effect as linear, and (3) modeling its effect as non-linear using a cubic spline smoother.

We used the absolute difference between the clinical test-based trend and the wastewater-based estimate as the response variable. We assumed its distribution to be either Gaussian or from the generalized normal family.⁵ In both cases, we modeled both the mean and variance parameters.

We performed model fitting in successive steps using the `gamlss` R package.⁶ We began by fitting a baseline model with a constant mean, then proceeded to fit the full model by first estimating the mean structure and subsequently modeling the variance. To compare and select the best-fitting model, we used the Akaike Information Criterion (AIC, [35]).

$$f(y|\mu, \sigma, \nu) = \frac{1}{\sqrt{2\pi}\sigma\mu^{\nu/2}} \exp \left[-\frac{1}{2} \frac{(y - \mu)^2}{\sigma^2\mu^{\nu}} \right] \quad (2)$$

⁶ <https://cran.r-project.org/web/packages/gamlss/index.html>

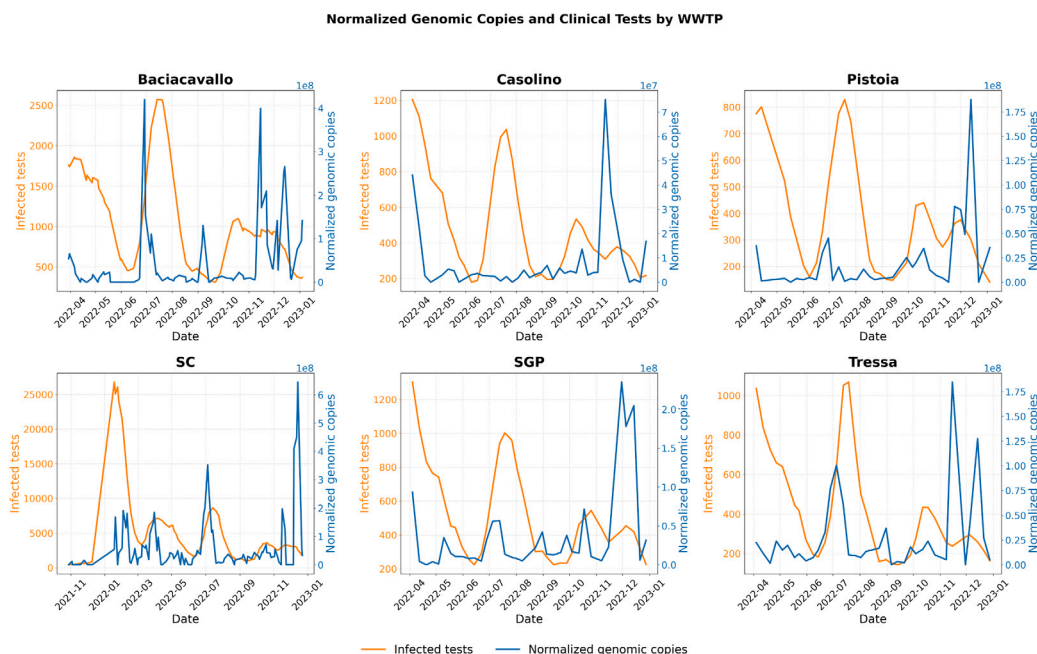


Fig. 1. Comparison between clinical test data and SARS-CoV-2 concentration normalized by daily average flow rate for all the 6 plants: Baciacavallo, Casolino, Pistoia, San Colombano (SC), San Giovanni Pianetto (SGP), Tressa.

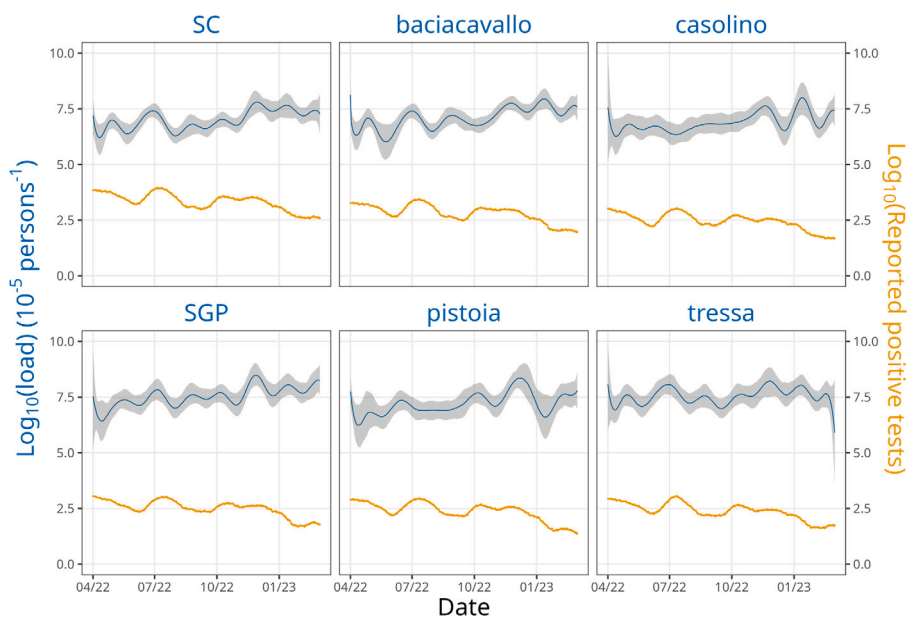


Fig. 2. Pooled model trends for all the 6 plants: San Colombano (SC), Baciacavallo, Casolino, San Giovanni Pianetto (SGP), Pistoia, Tressa.

3. Results and discussion

3.1. Spatial heterogeneity

The starting data, i.e. positive clinical tests and SARS-CoV-2 concentration in wastewater normalized by the daily average flow rate can be seen in Fig. 1. The detachment between the two data series that can be easily seen at the end of 2022 for all of the plants sparked our curiosity and led us to use a different model for our data, capable of pooling the plants together.

The model which describes the trend in each single plant as the sum of a regional trend and a plant-specific deviation fits the data well for most WWTPs, with a high proportion of observations falling within the 95% confidence interval: Baciacavallo (57.53%), Casolino

(92.5%), Pistoia (76.32%), San Colombano (75%), San Giovanni Pianetto (90.7%), and Tressa (85.37%). The notably lower performance observed at the Baciacavallo plant likely stems from the elevated proportion of industrial wastewater in its influent, particularly from the city of Prato's textile sector.

This strong model performance suggests that, despite plant-specific effects, the underlying pandemic trends are regionally consistent. Even when pooling all available data, we must note that 58% of the days in the selected timeframe lack measurements from any of the plants, highlighting the challenge of incomplete temporal coverage. We present the fitted trends for each WWTP in Fig. 2.

These results confirm that the model successfully captures the structure of the available data. It must be noted, as can be seen by the scatterplot in Fig. 4, that the model fails to explain much of the

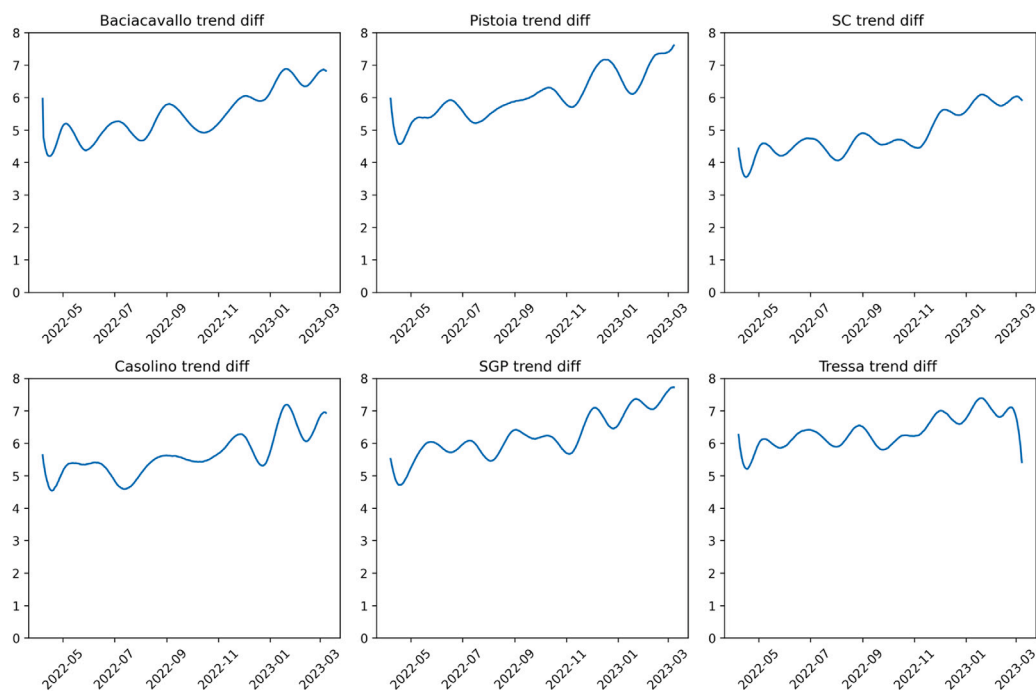


Fig. 3. Time series of the absolute difference between viral load and the base 10 logarithm of reported cases for all plants.

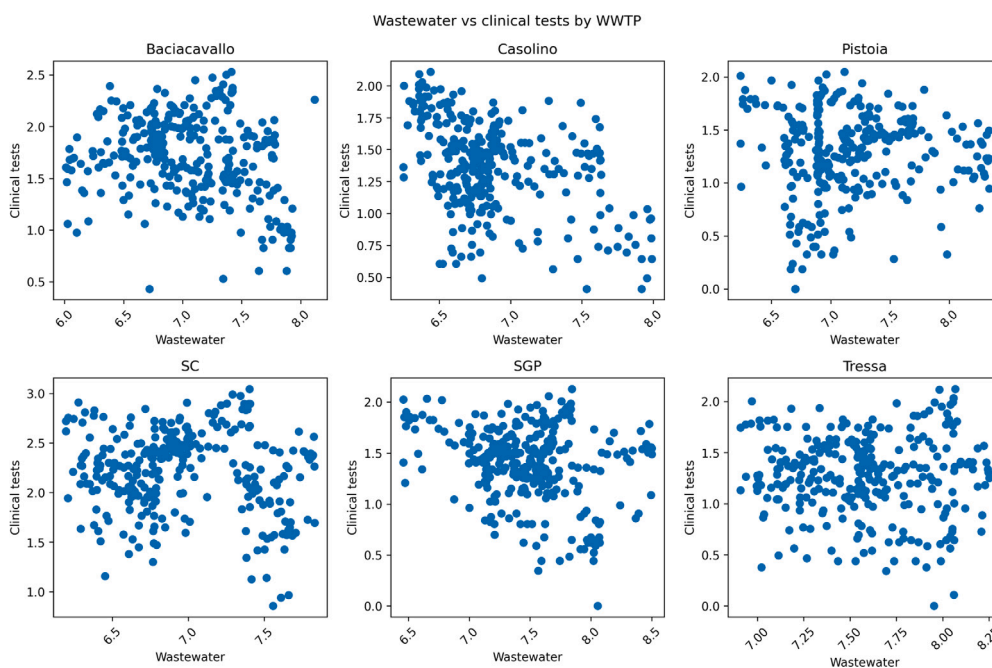


Fig. 4. Scatter plot with the model prediction and the positive clinical test, plant by plant. We can notice how there is always a gap between the two, still they are in the same magnitude order. The relationship is clearly non linear, and much of the variance present in the clinical test data is not explained by the model.

variability in the system. The inability of the model to account for the variance observed in clinical testing data provides further evidence that wastewater measurements and positive clinical test differ over the considered time window. While the model is capable of accurately fitting and describing wastewater trends, this alone is insufficient to reproduce the dynamics of positive clinical test results. This divergence indicates that the two data sources capture distinct aspects of the COVID-19 pandemic, thereby giving rise to the discrepancy that constitutes the focus of this study. In addition, despite the good fit, the model outputs clearly indicate a lack of correlation between wastewater and clinical

testing trends. To further investigate whether this misalignment could be explained by a temporal lag between the two signals, we performed a cross-correlation analysis.

We observed two key features in the data:

1. Similar to the clinical test trends, the wastewater-derived trends display consistent patterns across all plants. This regional coherence suggests that the drivers behind the discrepancies are not tied to individual plant characteristics but are instead shared across the Tuscany region.

Table 1

Spearman correlation with the absolute difference between clinical tests trend and wastewater trend resulting from the Hetebrji et al. model, all p-values are highly significant and $\ll 0.05$.

Value	Baciacavallo	Pistoia	San Colombano	Casolino	San Giovanni Pianetto	Tressa
confirmed cases	-0.42	-0.44	-0.37	-0.53	-0.46	-0.39
num of tests	-0.48	-0.49	-0.45	-0.54	-0.49	-0.40
positive ratio	-0.32	-0.34	-0.26	-0.48	-0.37	-0.35
rain [mm]	0.35	0.29	0.23	0.28	0.24	0.25
Other	0.47	0.24	0.46	0.25	0.43	0.42
Unknown	-0.55	-0.61	-0.46	-0.56	-0.56	-0.44
B.1.617.2 ^a	-0.49	-0.50	-0.45	-0.41	-0.46	-0.42
BA.1	-0.49	-0.55	-0.41	-0.50	-0.42	-0.46
BA.2	-0.52	-0.69	-0.47	-0.58	-0.56	-0.30
BA.2.75	0.78	0.82	0.74	0.77	0.76	0.66
BA.4	-0.39	-0.30	-0.29	-0.45	-0.29	-0.25
BA.5	0.08	0.13	0.04	0.06	0.09	-0.01
BQ.1	0.72	0.81	0.70	0.74	0.71	0.62
XBB	0.63	0.74	0.59	0.70	0.58	0.58
XBB.1.5	0.71	0.64	0.71	0.52	0.70	0.70

^a Only subvariant of the Delta family.

- Both the absolute and relative differences between the wastewater and clinical estimates vary over time. This time dependence implies that the underlying factors contributing to the discrepancy are temporally dynamic.

These observations guided our selection of explanatory variables for the GAMM, as any candidate feature must exhibit both spatial uniformity and temporal variability to plausibly explain the observed divergence.

To complement this analysis, we applied a linearly penalized segmentation algorithm [36], implemented via the *ruptures* Python package [37], to identify structural changes in the time series of absolute differences. This procedure revealed two prominent breakpoints that appeared consistently across most WWTPs: 20 August 2022 and 2 January 2023. Interestingly, both dates occur approximately one month after shifts in the dominant circulating SARS-CoV-2 subvariant.

3.2. Correlation test

To identify the variables driving the divergence between wastewater and clinical data, we conducted correlation analyses between the absolute difference in trend estimates and a set of explanatory features. These included clinical testing metrics such as the base-10 logarithm of the number of tests performed, the positivity rate, and their ratio, as well as viral subvariant prevalence. Results for the absolute difference are reported in Table 1.

All clinical testing variables showed negative correlation with the absolute difference, indicating that improved testing accuracy, reflected in higher testing volumes and lower positivity rates, reduces the discrepancy between clinical and wastewater signals. The Omicron variant, considered as a whole, also showed an overall negative correlation with the difference. However, this trend did not hold uniformly across all subvariants. Several subvariants, namely BA.2.75, BQ.1, XBB, and XBB.1.5, exhibited strong positive correlations with the absolute difference, suggesting that their emergence contributed to greater misalignment between the two trends. These virus-related variables also showed stronger correlations, in absolute terms, than any of the clinical testing features.

By comparing these correlations with the prevalence time series, we observed that subvariants peaking later in the study period tended to show positive correlations. Our literature-based hypothesis is that this pattern may reflect differences in viral shedding: subvariants that induce higher viral loads in infected individuals result in greater excretion of genomic material, leading to higher concentrations detected at the WWTP inlet [24,25]. Reduced viral load may also stem from host-related factors, such as vaccine-induced immunity, as well as inherent characteristics of the viral strain.

Analyses using the relative difference as the response variable produced comparable results concerning the subvariants. Clinical testing features slightly increased their correlations in absolute value, although they remained weaker than those associated with viral subvariant prevalence.

3.3. GAMM model results

Tables 2 and 3 report the coefficients estimated by the GAMM for the mean and variance components, respectively. Figs. 5 and 6 illustrate the model fits for each plant.

Based on the AIC, we selected a generalized normal distribution for modeling the response in three WWTPs, Baciacavallo, San Colombano, and San Giovanni Pianetto, and a standard Gaussian distribution for the remaining plants. Notably, only Pistoia exhibited signs of multimodality in the distribution of the absolute differences. We are, unfortunately, currently not able to explain the root cause of this multimodality.

Across most plants, subvariant-related predictors contributed more substantially to modeling the mean of the response, while clinical testing features had greater influence on the variance. This pattern seemingly reinforces the interpretation that viral subvariants introduce systematic effects: by altering the viral load produced by infected individuals and influencing RNA degradation dynamics in the sewage environment, different subvariants systematically shift the concentration measured at the WWTP inlet. In contrast, clinical testing quality primarily affects the variability of the clinical tests signal. This reinforces the knowledge that we are comparing wastewater with a source that has its own noise and error.

Some exceptions stand out. The BA.1 subvariant significantly influences both the mean and variance, indicating a broader impact on measurement alignment. Meanwhile, XBB primarily affects the mean. Interestingly, subvariants such as BA.2, BA.4, BA.5, and BQ.1 do not show significant effects in the GAMM, despite prior correlation analysis suggesting a meaningful role in at least some cases (notably BA.2 and BQ.1). This discrepancy highlights the value of modeling approaches like GAMM, which can account for the joint influence of multiple factors and help distinguish spurious associations from robust effects.

3.4. Limitations

The main limitations to our study come from the coarseness of the dataset. The wastewater data used in this study were not collected on a daily basis, but rather at weekly or biweekly intervals depending on the WWTP. This temporal resolution likely constrains our ability to detect

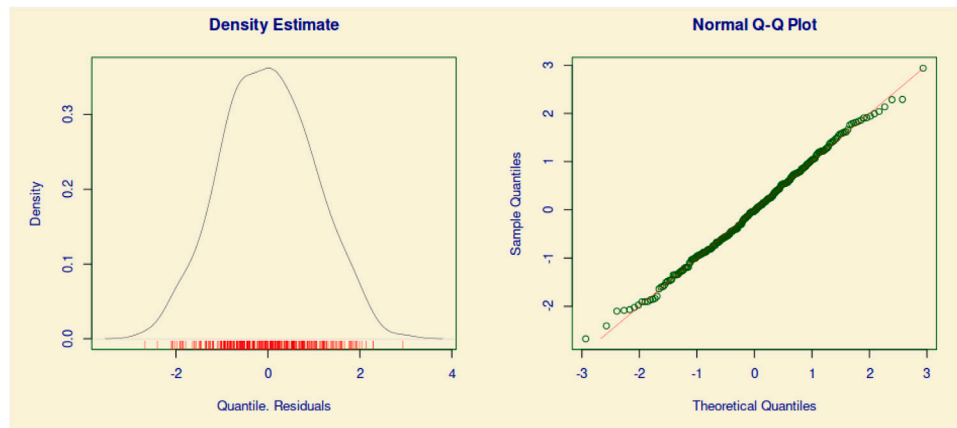


Fig. 5. Fit results for the GAMM applied to Baciacavallo WWTP. The density estimate validates the Gaussian hypothesis for the difference distribution, and the QQ-plot certifies the goodness of the fit.

Table 2
GAMM coefficients — mean.

Value	Baciacavallo	Pistoia	San Colombano	Casolino	San Giovanni Pianetto	Tressa
num of positives	< 0.1	< 0.1	X	< 0.1	X	X
num of tests	X	X	X	X	< 0.1	< 0.1
positive ratio	X	X	0.18	-0.14 ^a	X	X
Other	X	X	-0.10	X	-0.65	< 0.1
Unknown	< 0.1 ^a	X	-0.63 ^a	-0.17 ^a	-1.24 ^a	X
B.1.617.2 ^b	-2.5 ^a	X	X	X	0.48	-1.05 ^a
BA.1	X	0.2 ^a	-0.18 ^a	0.21 ^a	-0.21	X
BA.2	X	X	X	X	X	X
BA.2.75	0.15 ^a	0.15	< 0.1 ^a	< 0.1 ^a	-0.17 ^a	< 0.1
BA.4	X	X	X	< 0.1 ^a	< 0.1	< 0.1 ^a
BA.5	< 0.1 ^a	X	< 0.1 ^a	X	X	X
BQ.1	X	< 0.1 ^a	< 0.1	< 0.1	< 0.1 ^a	< 0.1 ^a
XBB	X	X	X	X	X	-0.37
XBB.1.5	X	X	X	0.16 ^a	X	X

X means the feature is not selected in the best model.

^a Variable is smoothed by cubic spline in best model.

^b Only subvariant of the Delta family.

Table 3
GAMM coefficients — variance.

Value	Baciacavallo	Pistoia	San Colombano	Casolino	San Giovanni Pianetto	Tressa
num of positives	X	-0.60	X	-1.01	-0.92	-0.94
num of tests	-1.08	X	-0.56	X	X	X
positive ratio	X	X	X	X	X	X
Other	X	X	X	-2.08	X	X
Unknown	X	X	X	X	X	X
B.1.617.2 ^b	X	X	X	4.90 ^a	X	-4.92
BA.1	0.46 ^a	0.28 ^a	< 0.1 ^a	X	0.33 ^a	0.26
BA.2	X	-0.23 ^a	X	X	X	X
BA.2.75	< 0.1 ^a	X	X	X	X	-0.28 ^a
BA.4	X	< 0.1 ^a	X	X	< 0.1 ^a	X
BA.5	< 0.1 ^a	X	X	< 0.1 ^a	X	< 0.1
BQ.1	X	X	X	< 0.1 ^a	X	X
XBB	X	X	< 0.1	-1.07	X	0.53 ^a
XBB.1.5	< 0.1 ^a	X	X	X	-0.35 ^a	X

X means the feature is not selected in the best model.

^a Variable is smoothed by cubic spline in best model.

^b Only subvariant of the Delta family.

potential time lags between wastewater signals and clinical testing data. In the present analysis, no such lag was identified; however, this outcome may be attributable to the limited sampling frequency, and different results might emerge with daily observations. It should be noted that the absence of an observed lag does not necessarily imply the true absence of such a lag, which may have implications for the selection of the same-day difference as the response variable in our

GAMM. Nevertheless, given the available data, this definition of the difference appeared to be the most appropriate choice.

Furthermore, it remains unclear whether this sampling scheme amplifies certain sources of noise or attenuates others. For example, the impact of rainfall is probably not adequately represented at this coarseness. This may be the reason behind our GAMM excluding precipitation data. It must be noted, however, that many wastewater

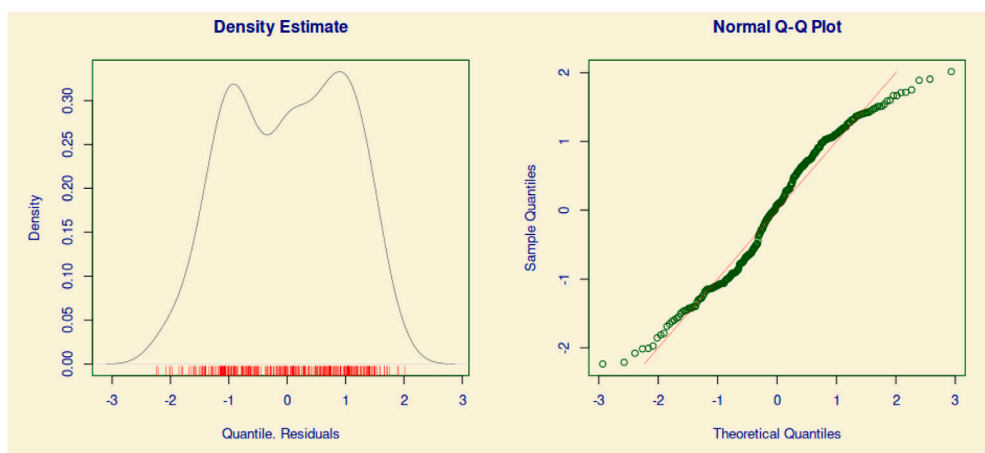


Fig. 6. Fit results for the GAMM applied to Pistoia WWTP. The density estimate shows some multimodality. The QQ-plot shows the presence of outliers.

datasets share similar temporal limitations, and thus may benefit from the considerations discussed herein. Consequently, this study may serve as a cautionary reference even for analyses based on higher-resolution data.

The scope of the model is further constrained by the availability of subvariant prevalence data from the ECDC, which are only reported up to January 2023, thereby excluding the final two months of the observation period. Nevertheless, there is no a priori reason to expect substantially different model behavior during the omitted interval. In addition, because the data are aggregated at the national level, the estimation of catchment area-level measures requires the assumption of spatial homogeneity. However, the prevalence of viral variants may display substantial geographic heterogeneity, potentially undermining this assumption.

The number of positive clinical tests was derived from coarse-grained data, as described in Section 2.2. The assumption of a spatially homogeneous epidemic introduces an additional approximation that may influence the results. However, within the time window considered, this effect is expected to be negligible in the context of the COVID-19 pandemic.

4. Conclusions

This study highlights the challenges inherent in designing and interpreting WBE surveillance systems, particularly when used to track infectious disease dynamics such as those of COVID-19. While WBE offers clear advantages over clinical testing, most notably lower costs and reduced logistical demands, it introduces its own complexities that must be rigorously accounted for in both study design and data interpretation.

Our analysis reveals that the relationship between viral genome concentrations of SARS-CoV-2 in wastewater measured in Tuscany in 2022 and 2023 and clinical case counts is neither constant nor straightforward. This relationship varies over time and is sensitive to multiple sources of noise. Some of these, such as population variability or rainfall-driven dilution, can be partially mitigated through normalization strategies. However, our results show that other confounding factors, particularly the prevalent viral subvariant and clinical test accuracy, significantly influence the alignment between wastewater and clinical trends.

While precedent work was able to show the presence of factors relative to viral variants and clinical tests, our work focuses on quantifying the influence of specific clinical and virological features. We found that clinical test performance, proxied by the positivity ratio, primarily affects the variance of the discrepancy, whereas viral subvariants more directly shift the mean. These findings better highlight

and define how each component affects the relationship between the RNA concentration measured in wastewater and clinical tests.

A novel contribution of our study is the incorporation of subvariant prevalence into the modeling pipeline, an approach not commonly implemented in WBE research. Our results demonstrate that subvariant dynamics, and not only variant of concern dynamics, substantially affect the wastewater signal and should be routinely monitored and incorporated into future models to maintain accuracy over time. Consequently, WBE systems must be flexible and adaptive, regularly updated to reflect virological evolution and shifting public health contexts.

Therefore, we advocate for a holistic surveillance framework that integrates wastewater data with other data sources such as clinical testing, genomic surveillance, and behavioral indicators, to enhance trend estimation and public health decision-making. Within such a framework, WBE functions not as a replacement but as a complementary signal, particularly valuable when traditional testing capacity is reduced.

In sum, this work represents an important step toward disentangling the multiple overlapping sources of noise in WBE data. By clarifying the role of clinical accuracy and viral subvariants, we offer a more grounded basis for interpreting wastewater signals and improving future modeling efforts. We hope that our findings will inform the development of more robust, responsive WBE frameworks capable of supporting ongoing and future epidemic monitoring.

CRedit authorship contribution statement

Daniele Sartirano: Writing – review & editing, Writing – original draft, Software, Methodology, Formal analysis, Data curation, Conceptualization. **Niel Hens:** Writing – review & editing, Supervision, Methodology, Conceptualization. **Claudio Lubello:** Writing – review & editing, Supervision, Conceptualization.

Declaration of generative AI and AI-assisted technologies in the manuscript preparation process

During the preparation of this work the author(s) used ChatGPT in order to rephrase part of the text. After using this tool/service, the author(s) reviewed and edited the content as needed and take(s) full responsibility for the content of the published article.

Declaration of competing interest

The authors declare that they have no known competing financial interests or personal relationships that could have appeared to influence the work reported in this paper.

Acknowledgments

Co-funded by the European Union - NextGenerationEU - National Recovery and Resilience Plan, Mission m, 4 Component 2 - Investment 1.5 - THE - Tuscany Health Ecosystem - ECS00000017 - CUP B83C22003920001. This study was supported by the Special Research Fund (BOF) of Hasselt University, grant letter R-14409 BOF24BL09. The authors also would like to thank Emanuele Massaro (European Environment Agency) and Daniela Paolotti (ISI Foundation) for the fruitful discussions.

Appendix A. Analysis with deceased

Given the central importance of the inaccuracies affecting clinical tests, we tried to replicate the model using an alternative data source, namely the proportion of deceased individuals within the population. This data source is expected to be less influenced by variations in the general population's willingness to undergo clinical testing. The relationship between RNA concentrations measured in wastewater and mortality is less direct than the association used in the GAMM approach described in this paper. Nevertheless, because our analysis focuses on trends rather than absolute values, the assumption that the difference between the two data sources should remain constant over time if their trends align continues to hold.

A.1. Deceased data and new GAMM

The mortality data are available in the same repository as the clinical test data, but they are aggregated at the regional level. Specifically, the figures represent the cumulative number of COVID-19-related deaths recorded across the entire Tuscany region up to each given day. To estimate the number of newly deceased individuals on a specific day, we computed the difference between the cumulative totals of consecutive days.

To derive estimates for each WWTP, we assumed that mortality was uniformly distributed across the region. Accordingly, the ratio of newly deceased individuals associated with each WWTP was calculated as

$$d_p(t) = \frac{(D(t) - D(t-1)) * pop_p}{pop_T} \quad (A.1)$$

where $d_p(t)$ denotes the ratio of newly deceased individuals for plant p on day t ,

$D(t)$ is the total number of deceased recorded in Tuscany on day t ,

pop_p represents the population served by plant p ,

and pop_T is the total population of the Tuscany region.

No correction was applied to account for the temporal delay between clinical testing and mortality. The difference used for the GAMM was the absolute difference between the mortality-based estimates and those obtained from the Hetebrji et al. model. The GAMM was constructed and fitted in the same manner as described in the main paper, with this new difference serving as the target function. The assumed distribution of the difference was again Gaussian.

A.2. Results and discussion

Tables B.4 and B.5 present the coefficients estimated by the GAMM for the mean and variance components, respectively. Figs. B.7 and B.8 display the model fits for the same plants reported in the original GAMM analysis.

Although multimodality is clearly not a concern, the model exhibits notable difficulty in accurately fitting and describing the observed differences. Regarding the estimated coefficients, the distinction between viral subvariants and features related to clinical tests, which were previously observed as primarily influencing the mean and variance of the distribution respectively, is less evident. Proxies for clinical test accuracy receive relatively larger coefficients even in the estimation of the mean, emphasizing their continued importance. Conversely, the influence of viral subvariants appears diminished, contributing less to the estimation of both the mean and the variance.

This finding, while subject to caution due to the limited quality of the model fit, is nonetheless noteworthy. It is unexpected that biases in clinical testing appear to exert a stronger effect even when mortality data are used, given that such biases should, in principle, have a much smaller impact on the number of deceased individuals than on the number of clinical tests.

Appendix B. Tables & figures

See Tables B.4 and B.5.

See Figs. B.7 and B.8.

Data availability

The data that has been used is confidential.

Table B.4
GAMM coefficients for deceased model — mean.

Value	Baciacavallo	Pistoia	San Colombano	Casolino	San Giovanni Pianetto	Tressa
num of positives	< 0.1	X	-0.61	X	-0.1	< 0.1
num of tests	X	-0.13	X	< 0.1	X	-0.15
positive ratio	X	0.22 ^a	-0.42 ^a	X	-0.16 ^a	X
Other	X	-0.16 ^a	X	-0.14 ^a	X	-0.13
Unknown	X	< 0.1 ^a	X	X	X	< 0.1 ^a
B.1.617.2 ^b	X	-0.51	X	X	X	-0.64
BA.1	X	< 0.1	< 0.1	< 0.1	< 0.1 ^a	X
BA.2	X	X	X	X	X	X
BA.2.75	X	< 0.1 ^a	< 0.1	< 0.1 ^a	< 0.1 ^a	< 0.1 ^a
BA.4	< 0.1 ^a	< 0.1 ^a	< 0.1 ^a	< 0.1 ^a	< 0.1 ^a	< 0.1 ^a
BA.5	X	X	X	X	X	X
BQ.1	X	< 0.1	X	X	X	< 0.1
XBB	X	X	0.14	< 0.1	X	X
XBB.1.5	< 0.1	X	X	X	-0.19	X

X means the feature is not selected in the best model.

^a Variable is smoothed by cubic spline in best model.

^b Only subvariant of the Delta family.

Table B.5
GAMM coefficients for deceased model — variance.

Value	Baciacavallo	Pistoia	San Colombano	Casolino	San Giovanni Pianetto	Tressa
num of positives	X	X	X	X	X	-0.65 ^a
num of tests	X	-0.46	X	-0.48 ^a	-0.98 ^a	X
positive ratio	X	X	X	X	2.76	X
Other	X	X	X	X	X	X
Unknown	X	X	X	X	X	X
B.1.617.2 ^b	X	X	X	X	X	X
BA.2	X	X	< 0.1	X	X	X
BA.2.75	X	0.1	X	0.18 ^a	X	0.27
BA.4	X	X	X	X	X	X
BA.5	X	X	X	X	X	X
BQ.1	X	X	X	< 0.1	X	X
XBB	X	-0.19 ^a	X	-0.57	X	-0.32
XBB.1.5	X	-0.27 ^a	X	X	X	-0.49 ^a

X means the feature is not selected in the best model.

^a Variable is smoothed by cubic spline in best model.

^b Only subvariant of the Delta family.

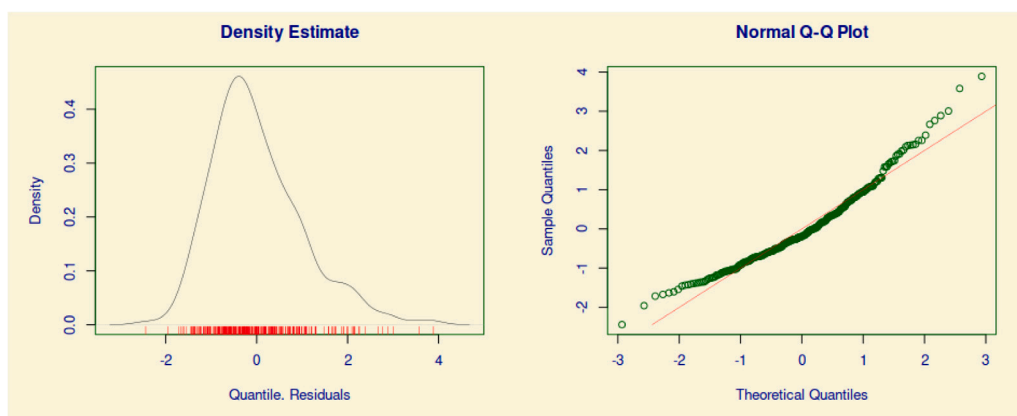


Fig. B.7. Fit results for the GAMM using the deceased as benchmark applied to Baciacavallo WWTP. The density estimate validates the Gaussian hypothesis for the difference distribution, and the QQ-plot signals the presence of outliers at the tails of the distribution.

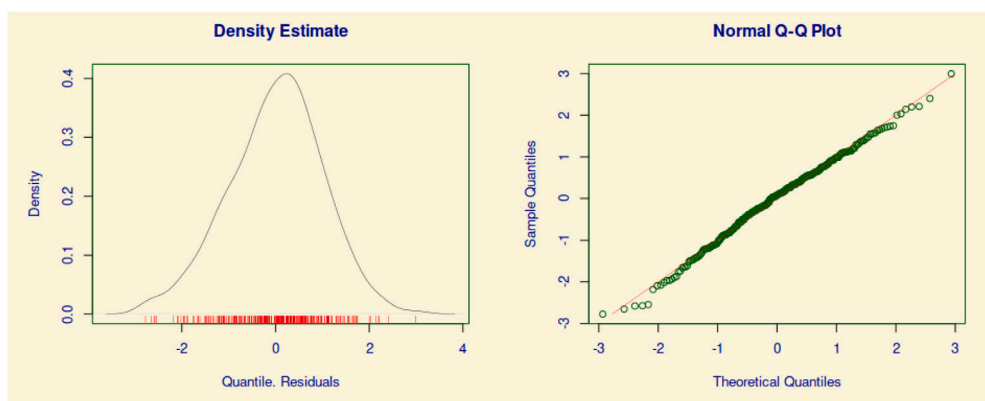


Fig. B.8. Fit results for the GAMM using the deceased as benchmark applied to Pistoia WWTP. The density estimate validates the Gaussian hypothesis for the difference distribution, and the QQ-plot certifies the goodness of the fit.

References

- [1] W. Ahmed, B. Tschärke, P.M. Bertsch, K. Bibby, A. Bivins, P. Choi, L. Clarke, J. Dwyer, J. Edson, T.M.H. Nguyen, J.W. O'Brien, S.L. Simpson, P. Sherman, K.V. Thomas, R. Verhagen, J. Zaugg, J.F. Mueller, SARS-CoV-2 RNA monitoring in wastewater as a potential early warning system for COVID-19 transmission in the community: A temporal case study, *Sci. Total Environ.* 761 (2021) 144216, <http://dx.doi.org/10.1016/j.scitotenv.2020.144216>.
- [2] M. Kumar, M. Joshi, A.K. Patel, C.G. Joshi, Unravelling the early warning capability of wastewater surveillance for COVID-19: A temporal study on SARS-CoV-2 RNA detection and need for the escalation, *Environ. Res.* 196 (2021) 110946, <http://dx.doi.org/10.1016/j.envres.2021.110946>.
- [3] N. Trigo-Tasende, J.A. Vallejo, S. Rumbo-Feal, K. Conde-Pérez, M. Vaamonde, A. López-Oriona, I. Barbeito, M. Nasser-Ali, R. Reif, B.K. Rodiño-Janeiro, E. Fernández-Álvarez, I. Iglesias-Corrás, B. Freire, J. Tarrío-Saavedra, L. Tomás, P. Gallego-García, D. Posada, G. Bou, I. López-de Ullibarri, R. Cao, S. Ladra, M. Poza, Wastewater early warning system for SARS-CoV-2 outbreaks and variants in a Coruña, Spain, *Environ. Sci. Pollut. Res.* 30 (32) (2023) 79315–79334, <http://dx.doi.org/10.1007/s11356-023-27877-3>.
- [4] Z.W. LaTurner, D.M. Zong, P. Kalvapalle, K.R. Gamas, A. Terwilliger, T. Crosby, P. Ali, V. Avadhanula, H.H. Santos, K. Weesner, L. Hopkins, P.A. Piedra, A.W. Maresso, L.B. Stadler, Evaluating recovery, cost, and throughput of different concentration methods for SARS-CoV-2 wastewater-based epidemiology, *Water Res.* 197 (2021) 117043, <http://dx.doi.org/10.1016/j.watres.2021.117043>, URL:

- <https://www.sciencedirect.com/science/article/pii/S0043135421002414>.
- [5] O.E. Hart, R.U. Halden, Computational analysis of SARS-CoV-2/COVID-19 surveillance by wastewater-based epidemiology locally and globally: Feasibility, economy, opportunities and challenges, *Sci. Total Environ.* 730 (2020) 138875, <http://dx.doi.org/10.1016/j.scitotenv.2020.138875>.
 - [6] L. Hopkins, D. Persse, K. Caton, K. Ensor, R. Schneider, C. McCall, L.B. Stadler, Citywide wastewater SARS-CoV-2 levels strongly correlated with multiple disease surveillance indicators and outcomes over three COVID-19 waves, *Sci. Total Environ.* 855 (2023) 158967, <http://dx.doi.org/10.1016/j.scitotenv.2022.158967>.
 - [7] X. Li, S. Zhang, S. Sherchan, G. Orive, U. Lertxundi, E. Haramoto, R. Honda, M. Kumar, S. Arora, M. Kitajima, G. Jiang, Correlation between SARS-CoV-2 RNA concentration in wastewater and COVID-19 cases in community: A systematic review and meta-analysis, *J. Hazard. Mater.* 441 (2023) 129848, <http://dx.doi.org/10.1016/j.jhazmat.2022.129848>.
 - [8] J. Peccia, A. Zulli, D.E. Brackney, N.D. Grubaugh, E.H. Kaplan, A. Casanovas-Massana, A.I. Ko, A.A. Malik, D. Wang, M. Wang, J.L. Warren, D.M. Weinberger, W. Arnold, S.B. Omer, Measurement of SARS-CoV-2 RNA in wastewater tracks community infection dynamics, *Nature Biotechnol.* 38 (10) (2020) 1164–1167, <http://dx.doi.org/10.1038/s41587-020-0684-z>.
 - [9] J. Weidhaas, Z.T. Aanderud, D.K. Roper, J. VanDerslice, E.B. Gaddis, J. Ostermiller, K. Hoffman, R. Jamal, P. Heck, Y. Zhang, K. Torgersen, J.V. Laan, N. LaCross, Correlation of SARS-CoV-2 RNA in wastewater with COVID-19 disease burden in sewersheds, *Sci. Total Environ.* 775 (2021) 145790, <http://dx.doi.org/10.1016/j.scitotenv.2021.145790>.
 - [10] A. Tiwari, A. Lippinen, A.-M. Hokajärvi, O. Luomala, A. Sarekoski, A. Rytönen, P. Österlund, H. Al-Hello, A. Juutinen, I.T. Miettinen, C. Savolainen-Kopra, T. Pitkänen, Detection and quantification of SARS-CoV-2 RNA in wastewater influent in relation to reported COVID-19 incidence in Finland, *Water Res.* 215 (2022) 118220, <http://dx.doi.org/10.1016/j.watres.2022.118220>.
 - [11] Council of European Union, Council regulation (EU) no 2024/3019, 2024, <http://data.europa.eu/eli/dir/2024/3019/oj>.
 - [12] N.K. Ibrahim, Epidemiologic surveillance for controlling Covid-19 pandemic: types, challenges and implications, *J. Infect. Public Health* 13 (11) (2020) 1630–1638, <http://dx.doi.org/10.1016/j.jiph.2020.07.019>.
 - [13] The COVID-19 testing debacle, *Nature Biotechnol.* 38 (6) (2020) <http://dx.doi.org/10.1038/s41587-020-0575-3>, 653–653.
 - [14] R. Maal-Bared, Y. Qiu, Q. Li, T. Gao, S.E. Hrudehy, S. Bhavanam, N.J. Ruecker, E. Ellehoj, B.E. Lee, X. Pang, Does normalization of SARS-CoV-2 concentrations by pepper mild mottle virus improve correlations and lead time between wastewater surveillance and clinical data in Alberta (Canada): comparing twelve SARS-CoV-2 normalization approaches, *Sci. Total Environ.* 856 (2023) 158964, <http://dx.doi.org/10.1016/j.scitotenv.2022.158964>.
 - [15] E. Symonds, K.H. Nguyen, V. Harwood, M. Breitbart, Pepper mild mottle virus: A plant pathogen with a greater purpose in (waste)water treatment development and public health management, *Water Res.* 144 (2018) 1–12, <http://dx.doi.org/10.1016/j.watres.2018.06.066>.
 - [16] J.S. Huisman, J. Scire, L. Caduff, X. Fernandez-Cassi, P. Ganesanandamoorthy, A. Kull, A. Scheidegger, E. Stachler, A.B. Boehm, B. Hughes, A. Knudson, A. Topol, K.R. Wigginton, M.K. Wolfe, T. Kohn, C. Ort, T. Stadler, T.R. Julian, Wastewater-based estimation of the effective reproductive number of SARS-CoV-2, *Environ. Health Perspect.* 130 (5) (2022) <http://dx.doi.org/10.1289/ehp10050>.
 - [17] A. Bivins, J. Greaves, R. Fischer, K.C. Yinda, W. Ahmed, M. Kitajima, V.J. Munster, K. Bibby, Persistence of SARS-CoV-2 in water and wastewater, *Environ. Sci. Technol. Lett.* 7 (12) (2020) 937–942, <http://dx.doi.org/10.1021/acs.estlett.0c00730>.
 - [18] W. Ahmed, P.M. Bertsch, K. Bibby, E. Haramoto, J. Hewitt, F. Huygens, P. Gyawali, A. Korajkic, S. Riddell, S.P. Sherchan, S.L. Simpson, K. Sirikanachana, E.M. Symonds, R. Verhagen, S.S. Vasani, M. Kitajima, A. Bivins, Decay of SARS-CoV-2 and surrogate murine hepatitis virus RNA in untreated wastewater to inform application in wastewater-based epidemiology, *Environ. Res.* 191 (2020) 110092, <http://dx.doi.org/10.1016/j.envres.2020.110092>.
 - [19] S. Nourbakhsh, A. Fazil, M. Li, C.S. Mangat, S.W. Peterson, J. Daigle, S. Langner, J. Shurgold, P. D'Aoust, R. Delatolla, E. Mercier, X. Pang, B.E. Lee, R. Stuart, S. Wijayarsi, D. Champredon, A wastewater-based epidemic model for SARS-CoV-2 with application to three Canadian cities, *Epidemics* 39 (2022) 100560, <http://dx.doi.org/10.1016/j.epidem.2022.100560>.
 - [20] C. McCall, Z.N. Fang, D. Li, A.J. Czubai, A. Juan, Z.W. LaTurner, K. Ensor, L. Hopkins, P.B. Bedient, L.B. Stadler, Modeling SARS-CoV-2 RNA degradation in small and large sewersheds, *Environ. Sci.: Water Res. Technol.* 8 (2) (2022) 290–300, <http://dx.doi.org/10.1039/d1ew000717c>.
 - [21] A. Xiao, F. Wu, M. Bushman, J. Zhang, M. Imakaev, P.R. Chai, C. Duvallet, N. Endo, T.B. Erickson, F. Armas, B. Arnold, H. Chen, F. Chandra, N. Ghaeli, X. Gu, W.P. Hanage, W.L. Lee, M. Matus, K.A. McElroy, K. Moniz, S.F. Rhode, J. Thompson, E.J. Alm, Metrics to relate COVID-19 wastewater data to clinical testing dynamics, *Water Res.* 212 (2022) 118070, <http://dx.doi.org/10.1016/j.watres.2022.118070>, URL: <https://www.sciencedirect.com/science/article/pii/S0043135422000331>.
 - [22] M.R.J. Varkila, M.E. Montez-Rath, J.A. Salomon, X. Yu, G.A. Block, D.K. Owens, G.M. Chertow, J. Parsonnet, S. Anand, Use of wastewater metrics to track COVID-19 in the US, *JAMA Netw. Open* 6 (7) (2023) <http://dx.doi.org/10.1001/jamanetworkopen.2023.25591>, e2325591–e2325591.
 - [23] R. Schill, K.L. Nelson, S. Harris-Lovett, R.S. Kantor, The dynamic relationship between COVID-19 cases and SARS-CoV-2 wastewater concentrations across time and space: Considerations for model training data sets, *Sci. Total Environ.* 871 (2023) 162069, <http://dx.doi.org/10.1016/j.scitotenv.2023.162069>.
 - [24] O. Puhach, B. Meyer, I. Eckerle, SARS-CoV-2 viral load and shedding kinetics, *Nat. Rev. Microbiol.* (2022) <http://dx.doi.org/10.1038/s41579-022-00822-w>.
 - [25] S.J.R.d. Silva, S.C.d. Lima, R.C.d. Silva, A. Kohl, L. Pena, Viral load in COVID-19 patients: Implications for prognosis and vaccine efficacy in the context of emerging SARS-CoV-2 variants, *Front. Med.* 8 (2022) <http://dx.doi.org/10.3389/fmed.2021.836826>.
 - [26] W.A. Hetebrj, A.M. de Roda Husman, E. Nagelkerke, R.F. van der Beek, S.C. van Iersel, T.G. Breuning, W.J. Lodder, M. van Boven, Inferring hospital admissions from SARS-CoV-2 virus loads in wastewater in The Netherlands, august 2020 – february 2022, *Sci. Total Environ.* 912 (2024) 168703, <http://dx.doi.org/10.1016/j.scitotenv.2023.168703>.
 - [27] T.J. Hastie, *Generalized additive models*, in: *Statistical Models in S*, Routledge, 2017, pp. 249–307.
 - [28] F. Morecchiato, M. Coppi, C. Niccolai, A. Antonelli, L. Di Gloria, P. Calà, F. Mancuso, M. Ramazzotti, T. Lotti, C. Lubello, G.M. Rossolini, Evaluation of different molecular systems for detection and quantification of SARS-CoV-2 RNA from wastewater samples, *J. Virol. Methods* 328 (2024) 114956, <http://dx.doi.org/10.1016/j.jviromet.2024.114956>.
 - [29] O. Gressani, J. Wallinga, C.L. Althaus, N. Hens, C. Faes, Epilps: A fast and flexible Bayesian tool for estimation of the time-varying reproduction number, in: C.J. Struchiner (Ed.), *PLoS Comput. Biol.* 18 (10) (2022) e1010618, <http://dx.doi.org/10.1371/journal.pcbi.1010618>.
 - [30] H. Lau, T. Khosrawipour, P. Kocbach, H. Ichii, J. Bania, V. Khosrawipour, Evaluating the massive underreporting and undertesting of COVID-19 cases in multiple global epicenters, *Pulmonology* 27 (2) (2021) 110–115, <http://dx.doi.org/10.1016/j.pulmoe.2020.05.015>.
 - [31] H. Rahmandad, T.Y. Lim, J. Sterman, Behavioral dynamics of <sc>sc>COVID-19: estimating underreporting, multiple waves, and adherence fatigue across 92 nations, *Syst. Dyn. Rev.* 37 (1) (2021) 5–31, <http://dx.doi.org/10.1002/sdr.1673>.
 - [32] E. Mehraeen, Z. Pashaei, F.K. Akhtarani, M. Dashti, A. Afzalani, A. Ghasemzadeh, P. Asili, M.S. Kahrizi, M. Mirahmad, E. Rahimi, P. Matini, A.M. Afsahi, O. Dadras, S. SeyedAlinaghi, Estimating methods of the undetected infections in the COVID-19 outbreak: A systematic review, *Infect. Disord. - Drug Targets* 23 (4) (2023) <http://dx.doi.org/10.2174/1871526523666230124162103>.
 - [33] M.H. Murad, N. Asi, M. Alsawas, F. Alahadab, New evidence pyramid, *BMJ Evidence-Based Med.* 21 (4) (2016) 125–127, <http://dx.doi.org/10.1136/ebmed-2016-110401>, URL: <https://ebm.bmj.com/content/21/4/125>.
 - [34] Italian Ministry of Health, Urgent dispositions for the overcoming of the measures contrasting the diffusion of the COVID-19 epidemic, due to the ceasing of the state of emergency. (22g00034) (GU general series n.70 of 24-03-2022) [disposizioni urgenti per il superamento delle misure di contrasto alla diffusione dell'epidemia da COVID-19, in conseguenza della cessazione dello stato di emergenza. (22g00034) (GU serie generale n.70 del 24-03-2022)], 2022.
 - [35] H. Akaike, B.N. Petrov, F. Csaki, Second international symposium on information theory, 1973.
 - [36] R. Killick, P. Fearnhead, I.A. Eckley, Optimal detection of changepoints with a linear computational cost, *J. Amer. Statist. Assoc.* 107 (500) (2012) 1590–1598, <http://dx.doi.org/10.1080/01621459.2012.737745>.
 - [37] C. Truong, L. Oudre, N. Vayatis, Selective review of offline change point detection methods, *Signal Process.* 167 (2020) 107299, <http://dx.doi.org/10.1016/j.sigpro.2019.107299>.